Published in final edited form as:
J Nucl Med. 2012 June ; 53(6): 961–968. doi:10.2967/jnumed.111.092361.

PET with ^{64}Cu–Histidine for Noninvasive Diagnosis of Biliary Copper Excretion in Long–Evans Cinnamon Rat Model of Wilson Disease

Ralf Bahde[1,2], **Sorabh Kapoor**[1,2], **Kuldeep K. Bhargava**[3,4], **Michael L. Schilsky**[5], **Christopher J. Palestro**[3,4], and **Sanjeev Gupta**[1,2]

[1]Marion Bessin Liver Research Center, Diabetes Center, and Cancer Research Center, Departments of Medicine and Pathology, Ruth L. and David S. Gottesman Institute for Stem Cell and Regenerative Medicine Research, Albert Einstein College of Medicine, Bronx, New York

[2]Einstein–Montefiore Institute for Clinical and Translational Research, Albert Einstein College of Medicine, Bronx, New York

[3]Division of Nuclear Medicine and Molecular Imaging, North Shore–Long Island Jewish Health System, New Hyde Park, New York

[4]Hofstra North Shore–LIJ School of Medicine, Hempstead, New York

[5]Yale–New Haven Transplantation Center, Yale School of Medicine, New Haven, Connecticut

Abstract

Excretion of copper into bile requires the copper transporter *Atp7b*, which is deficient in Wilson disease. We hypothesized that a radiocopper–histidine complex would be effective for diagnosing Wilson disease by molecular imaging and tested this hypothesis in the Long–Evans cinnamon (LEC) rat model with *Atp7b* deficiency.

Methods—We complexed ^{64}Cu to L-histidine and analyzed clearance from blood, uptake in tissues, and excretion in bile of healthy Long–Evans agouti (LEA) rats versus LEC rats modeling Wilson disease. Sixty-minute dynamic PET recordings were obtained in LEA and LEC rats. Possible effects of acute and chronic liver injury induced by carbon tetrachloride were studied in LEA rats. *Atp7b* deficiency in LEC rats was reconstituted by transplantation of healthy cells to establish the specificity of findings.

Results—Examination of blood, tissue, and bile showed that in healthy rats, radiocopper was incorporated in the liver, followed by rapid excretion in bile. Corresponding blood, tissue, and bile studies in LEC rats showed incorporation of radiocopper in the liver but without copper excretion in bile, leading to hepatic retention of the radiotracer. PET showed onset of copper clearance in the liver of LEA rats, whereas liver copper content progressively increased in LEC rats during the 1-h period. Hepatic radiocopper excretion was not altered by either acute or chronic liver injury. In LEC rats with liver repopulation by transplanted healthy hepatocytes, excretion of radiocopper confirmed that *Atp7b* was responsible for this effect.

For correspondence or reprints contact: Sanjeev Gupta, Albert Einstein College of Medicine, 1300 Morris Park Ave., Ullmann Building, Room 625, Bronx, NY 10461. sanjvgupta@pol.net, sanjeev.gupta@einstein.yu.edu.

DISCLOSURE STATEMENT
No other potential conflict of interest relevant to this article was reported.

Conclusion—Imaging with the radiocopper–histidine complex successfully identified *Atp7b*-dependent biliary copper excretion. This principle will advance molecular imaging for Wilson disease.

Keywords

Atb7b; positron emission tomography; radiocopper; Wilson disease

Copper is indispensable for life, but excessive amounts of copper are toxic. Wilson disease (WD) is characterized by copper toxicosis, with liver or brain damage (1). Molecular mechanisms in copper handling are complex (2). Failure of copper excretion due to genetic defects in biliary copper transporter *A* is central to WD (3).

Diagnosis of WD requires demonstration of increased liver copper content by liver biopsy (1). However, liver biopsy may be hazardous. Also, liver copper content is most reliably measured by atomic force spectroscopy, which is not widely available. On occasion, variations in tissue sampling and early stages of WD with less copper accumulation might confound diagnosis. Although genetic tests for WD are being developed, the *ATP7B* gene is large, with more than 200 disease-causing mutations, and correlations between these mutations and protein function is difficult.

Noninvasive diagnosis of WD, particularly at an early state, will be significant, because copper can be mobilized by drugs or possibly by cell or gene therapy approaches (1,4–7). Previously, diagnosis of WD with radiocopper was unsuccessful. Binding of ^{64}Cu to plasma ceruloplasmin proved irrelevant (8). Tests of ^{64}Cu excretion in urine or stool were ineffective (9–11), in part because free ^{64}Cu is widely distributed in the body, followed by gradual release and reuptake in organs over hours.

We hypothesized that delivery of radiotracers as suitable complexes capable of targeting organs could be helpful, for example, ^{64}Cu complexed to histidine, because administration of this complex led to biliary excretion of copper in an *Atp7b*-dependent manner (12). The structure, properties, and utility of copper–histidine for delivering copper to tissues have been established (13). Therefore, a copper–histidine complex could deliver radiocopper in suitable ionic states to plasma membranes, followed by physiologic intracellular processing, and biliary excretion by *ATP7B*. Normally, copper is incorporated in cells largely by Ctr1, a conserved protein with high affinity for copper import (2). Intracellular routing, secretion, or excretion of copper from cells includes distribution of Cu1+, for example, by a copper chaperone to superoxide dismutase-1, by unknown ligands to mitochondria, and by transfer by Atox1 chaperone to *ATP7A* on the basolateral membrane for secretion into blood or fluids and *ATP7B* for excretion into bile canaliculus (14). Therefore, we studied the ^{64}Cu–histidine complex in Long–Evans cinnamon (LEC) rats, in which the *Atp7b* gene is mutated, and their healthy counterparts, Long–Evans agouti (LEA) rats, in which *Atp7b* functions normally (4–6,15).

MATERIALS AND METHODS

Chemicals

L-histidine (H6034), sodium valproate (P4543), hydrocortisone (H0135), and reagents were from Sigma Chemical Co.

^{64}Cu–Histidine

We purchased ^{64}Cu-chloride, with a specific activity of 962 MBq/μg, along with ^{67}Cu (6%) and ^{67}Ga (0.8%), from MDS Nordion (catalog IPG-^{64}Cu). To 200 μg of L-histidine in 500

μL of 0.1 M 4-(2-hydroxyethyl)-1-piperazineethanesulfonic acid (HEPES), pH 7.4, we added 148–185 MBq of ^{64}Cu, incubated for 15 min at room temperature. ^{64}Cu–histidine was purified by being passed through Sep-Pak C18 cartridges (WAT023501; Waters Corp.). These were prewashed with 10 mL of ethanol, followed by 10 mL of water. After injection of ^{64}Cu–histidine, cartridges were washed with 5 mL of water. ^{64}Cu–histidine was eluted by 3 mL of ethanol from cartridges and yielded 136–170 MBq of activity. The specific activity of ^{64}Cu–histidine was 700–750 MBq/mg. The purity of ^{64}Cu–histidine complex was analyzed by instant thin-layer chromatography strips, with acetone as a solvent. The mobile phase was analyzed by dividing instant thin-layer chromatography strips and measuring activity in a well counter. ^{64}Cu–histidine was 95% pure or greater.

Animals

Animal Care and Use Committees and Radiation Safety at Albert Einstein College of Medicine and Feinstein Institute of Medical Research, North Shore–Long Island Jewish Health System, approved the protocols. LEA and LEC rats, 8–12 wk old and weighing 250–300 g, were from the Special Animal Core of Marion Bessin Liver Research Center. F344 rats, 8–24-wk old and weighing 250–300 g, were procured when younger from the National Cancer Institute.

Genotyping of LEC and LEA Rats

Animals were genotyped by polymerase chain reaction of genomic DNA, as described previously (16). Hepatic *Atp7b* messenger RNA (mRNA) was shown by reverse transcription polymerase chain reaction with RNA extracted by TRIzol reagent (Invitrogen). Primers were as follows. *Atp7b*: 5′-CCATCTCCAGTGATATCAGTG-3′ (forward); 5′-CGCACAGCACACCATCAATGG-3′ (reverse); rat β-actin: 5′-CCCTGGCTCCTAGCACCAT-3′ (forward) and 5′-AGAGCCACCAATCCACACAGA-3′ (reverse) (17).

Surgical Procedures

Rats were anesthetized with ketamine and xylazine (Fort Dodge Animal Health) or inhaled isoflurane. The common bile duct was isolated by laparotomy and cannulated with polyethylene-50 tubing (Becton Dickinson Labware). Spleen was isolated by subcostal incision. Hepatocytes were isolated by collagenase perfusion of liver, as described previously (4–6). For cell transplantation studies, homozygous LEC rats (LEC−/−) rats were given retrorsine (20 mg/kg) at 6 and 8 wk of age, with two-thirds partial hepatectomy 4 wk later, and 5×10^6 hepatocytes from donor LEA rats were injected intrasplenically (4).

Protocols for Biodistributions and Hepatic Handling of ^{64}Cu Complexes

For analyzing ^{64}Cu–histidine handling over up to 24 h, we collected blood from a tail cut every 15 min for 1 h and at 3 h and 24 h (Fig. 1). Bile was collected at 15-min intervals between 0 and 1 h and for 60 min before 3 and 24 h after injection of ^{64}Cu–histidine. Bile flow rates were 1.8 ± 0.4 mL per hour. Samples of liver, kidneys, spleen, heart, and lungs were collected, and total organ weights were obtained. Because ^{64}Cu contained 6% ^{67}Cu, blood, bile, and tissue samples were efficiently analyzed by γ-counting.

Radioactivity was measured simultaneously with decay correction in samples. Organ activity was expressed on a per-gram-of-tissue basis, with normalization against heart muscle for background, which was taken as zero activity. This activity was converted to the actual weight of whole organs. The extent of hepatic copper removal was determined by dividing counts in bile by counts in liver plus bile after 1 h, permitting comparison of changes in hepatic copper activity shown by small-animal PET.

For small-animal PET, animals were spread supine, and imaging was centered on the upper abdomen. Animals were anesthetized with isoflurane inhalation and kept warm. Image acquisitions began with 350- to 650-keV windows before 18.5 MBq of ^{64}Cu–histidine were injected (specific activity, 700–750 MBq/mg) (R4 Scanner; Concorde MicroSystems). Sixty-minute dynamic PET recording was performed in rats using 2-min frames (Fig. 1). Animals were reimaged after 3 and 24 h with single 10-min frames. Image analysis incorporated isotope decay, scatter, dead-time, and arc corrections (ASIPro software; Siemens Medical Solutions USA, Inc.). Hepatic regions of interest in equal volumes were selected at some distance from the liver edge and diaphragm to decrease respiratory artifacts. Standardized uptake values (SUVs) were plotted against time, and time-to-peak hepatic SUV was determined. Linear regression was used to determine changes in ^{64}Cu activity. In LEC rats, well-defined maximum SUV (SUVmax) was not observed.

Multiple animal groups were established for studies (Table 1). First, we established that peripheral injection via tail vein or intrasplenic injection of ^{64}Cu–histidine gave similar results in LEA, heterozygous LEC rats (LEC+/−) and LEC−/− rats. We preferred the intrasplenic route for convenience for ensuring delivery of radioisotope without extravasation. We injected 3.7–5.5 MBq of ^{64}Cu–histidine (specific activity, 700–750 MBq/mg), followed by 0.5 mL of saline flush. We included animals with liver injury and analyzed drug effects on bile copper excretion.

Induction of Liver Injury

For acute injury, we injected CCl_4 (1 mL/kg) in mineral oil (1:1, v/v) intraperitoneally once 3 d before studies (18,19). Chronic injury was induced by 0.5 g of phenobarbitone per liter in drinking water, along with CCl_4 (0.25–0.5 mL/kg) in mineral oil (1:1, v/v) intraperitoneally every 4–5 d for 3 mo (18).

^{99m}Tc-Mebrofenin Scintigraphy

Abcc2 transporter activity was demonstrated by imaging with its ligand, ^{99m}Tc-mebrofenin, as described previously (20).

Drug-Induced Bile Copper Excretion

To establish whether biliary excretion of ^{64}Cu–histidine could be increased by bile flow (21–23), we injected valproic acid (150 mg/kg) or hydrocortisone (10 mg/kg) intrasplenically before ^{64}Cu–histidine, followed by analysis of organ distribution and ^{64}Cu excretion in tissue samples and collected bile.

Histologic Analysis

Cryostat sections of 5-μm thickness were prepared from tissues frozen in methylbutane at −80°C. Acetone-fixed sections were stained with hematoxylin and eosin. Sections were fixed in chloroform–acetone (1:1, v/v) or in 4% paraformaldehyde and 85% ethanol for γ-glutamyl transpeptidase and myeloperoxidase, respectively, as described previously (24). To stain collagen, sections were fixed in absolute ethanol, followed by Sirius red staining with direct red 80 in saturated aqueous picric acid. Staining for α-smooth muscle actin was as described previously (25). For *Atp7b* staining, sections were fixed in 4% paraformaldehyde and incubated with 1:50 E12A antiserum (from Dr. Jonathan D. Gitlin) (26), followed by Alexa Fluor 488–conjugated goat antirabbit IgG (1:500, Molecular Probes). Nuclei were counterstained by 4′,6-diamidino-2-phenylindole.

Statistical Analysis

Data are expressed as mean ± SD. Analyses used *t* tests, Mann–Whitney rank sum tests, or ANOVA, including Holm–Sidak pairwise comparisons with SigmaStat 3.1 (Systat Inc.). *P* values less than 0.05 were considered significant.

RESULTS

Genotyping of Animals

Morphologically, the liver was normal in LEA rats and heterozygous LEC+/− rats (not shown). By contrast, homozygous LEC−/− rats showed enlarged hepatocytes, biliary proliferation, and fibrosis. Liver copper in LEA rats and LEC+/− rats was 20 ± 13 and 44 ± 38 μg/g ($n = 6$), respectively, and was less than liver copper in LEC−/− rats (860 ± 58 μg/g) ($n = 6$; $P < 0.001$). We confirmed that *Atp7b* mRNA was expressed in LEA and LEC+/− rats and not in LEC−/− rats.

^{64}Cu–Histidine Clearance from Blood and Tissues

Measurements of blood activity showed ^{64}Cu–histidine cleared gradually in LEA rats, because 74% ± 5% and 71% ± 9% of the activity after 15 min was still present at 45 min and 24 h, respectively (Fig. 2A). Clearance of ^{64}Cu– histidine from blood was similar in LEC+/− rats after 45 min, 75% ± 5%, although less activity remained after 24 h, 50% ± 12% ($P < 0.05$, ANOVA). LEC−/− rats cleared ^{64}Cu–histidine from the blood most efficiently, with 61% ± 5% activity remaining after 45 min and only 9% ± 2% after 24 h ($P < 0.05$, ANOVA). The analysis of excised organs showed that ^{64}Cu–histidine was largely in the liver, followed by kidneys, in all animal groups, which was in agreement with hepatic and renal targeting (Fig. 2B). Liver activity was greatest in LEC−/− rats ($P < 0.05$), correlating with more rapid blood clearance of ^{64}Cu–histidine in these animals. To examine whether biliary copper excretion accounted for differences in hepatic ^{64}Cu activity, we studied bile at 1, 3, and 24 h after ^{64}Cu–histidine injection (Fig. 2C). In LEA and LEA+/− rats, ^{64}Cu appeared in bile within 15 min. However, bile from LEC rats lacked ^{64}Cu activity, indicating that biliary excretion of ^{64}Cu in LEA and LEC+/− rats was due to *Atp7b*. Most ^{64}Cu was excreted within the first hour, such that in LEA rats and LEC+/− rats, 10% ± 5% of liver-plus-bile activity was in bile at that time (Fig. 2D). Also, in LEA and LEC+/− rats, liver ^{64}Cu activity declined in parallel with biliary copper excretion. For instance, in LEA rats, 52% ± 8% of activity in the first hour was in the liver after 24 h (Fig. 2E). This rate of clearance extrapolated to hourly losses of approximately 2% of ^{64}Cu activity beyond the first hour. Liver ^{64}Cu activity remained far greater at all times in LEC−/− rats than in LEA or LEC+/− rats ($P < 0.05$). Indeed, liver ^{64}Cu activity rose progressively in LEC−/− rats and increased from 1 to 24 h by 183% ± 69%, $P < 0.05$.

Small-Animal PET Studies to Identify ^{64}Cu Excretion

In all cases, dynamic liver imaging over 1 h after ^{64}Cu–histidine showed the liver (Fig. 3A). In LEA and LEC+/− rats, hepatic activity declined over time. By contrast, ^{64}Cu progressively accumulated in the liver of LEC−/− rats. In LEA rats, the time to peak hepatic SUV was 13 ± 2 min. Hepatic SUV declined in these rats by 10% ± 2% over 1 h (Fig. 3B). This number was consistent with loss of activity in liver tissue and appearance in bile. After 3 and 24 h in LEA rats, hepatic SUV declined by 13% ± 5% and 45% ± 6%, respectively, indicating further exit of ^{64}Cu from liver. This decrease in hepatic SUV also correlated with tissue and bile studies. By contrast, in LEC+/− rats, hepatic SUV increased progressively, including in the first hour itself.

Acute or Chronic Liver Injury Did Not Alter ^{64}Cu– Histidine Handling

In LEA rats 3 d after a single dose of CCl_4, liver histology confirmed acute injury, with changes of hepatic γ-glutamyl transpeptidase expression (as expected), inflammatory cell infiltrates, and inhibition of ^{99m}Tc-mebrofenin excretion (not shown). Despite acute liver injury in LEA rats, uptake of ^{64}Cu-histidine in organs was similar to that in healthy LEA rats. Also, the kinetics of bile ^{64}Cu excretion was similar to that in healthy LEA rats. Continued clearance of ^{64}Cu over time decreased hepatic activity after 24 h.

In rats treated with repeated CCl_4, liver histology indicated chronic injury with fibrosis and cirrhosis, as expected (Fig. 4A). Clearance of ^{64}Cu–histidine from the blood was lower in cirrhotic rats than in healthy rats. However, less ^{64}Cu activity in the liver was retained in cirrhotic rats than in LEC−/− rats (Fig. 4B). Moreover, cirrhotic rats excreted ^{64}Cu in bile, whereas LEC−/− rats excreted none (Fig. 4C).

Regulation of Biliary Copper Excretion by Drugs

We used sodium valproate and hydrocortisone because these drugs increased bile flow and were thought to increase copper excretion (21–23). Sodium valproate and hydrocortisone increased bile flow in LEA rats over 1 h by 132% ± 7% and 199% ± 52%, respectively, above untreated controls, $P < 0.05$. However, sodium valproate or hydrocortisone did not change ^{64}Cu excretion.

Biliary Copper Excretion After Atp7b Reconstitution in LEC Rats by Cell Transplantation

To substantiate the specificity of the small-animal PET approach, we examined whether reconstitution of *Atp7b* function will restore ^{64}Cu excretion in LEC rats. Therefore, we transplanted healthy LEA rat hepatocytes in LEC−/− rats under liver repopulation conditions and studied animals ($n = 10$) after 3, 7, 10, or 12mo. In 7 LEC−/− rats, cell transplantation was successful, with the lowering of liver copper content to 125 ± 66 μg/g, detection of *Atp7b* mRNA by reverse transcription polymerase chain reaction, identification of LEA rat hepatocytes by immunostaining for *Atp7b*, and excretion of ^{64}Cu in bile (Fig. 5). In 3 LEC−/− rats, liver was not repopulated, because liver copper content was high, *Atp7b* mRNA was absent, *Atp7b* immunostaining did not show LEA rat hepatocytes, and ^{64}Cu was not excreted in bile. Dynamic small-animal PET over 1 h showed that these animals handled copper differently. Hepatic SUV increased less in LEC−/− rats with liver repopulation and biliary excretion of ^{64}Cu than in LEC−/− rats with no liver repopulation and no biliary excretion of ^{64}Cu. In the latter situation, ^{64}Cu accumulated similarly to its accumulation in untreated LEC−/− rats, shown earlier. Therefore, *Atp7b* reconstitution in LEC−/− rats accounted for ^{64}Cu excretion, confirming the specificity of this small-animal PET approach in WD.

DISCUSSION

This study established that ^{64}Cu–histidine was appropriately distributed, incorporated, and processed with *Atp7b*-mediated biliary copper excretion in healthy rat liver, permitting diagnosis of the WD state in LEC rats. The specificity of the ^{64}Cu imaging approach was verified by *Atp7b* reconstitution in LEC rats. The imaging parameters based on hepatic clearance of ^{64}Cu should advance clinical diagnosis of WD. Also, distinctions between altered bile flow rates and copper excretion by imaging should facilitate drug development for mobilization and excretion of copper.

As a strong metal-coordinating ligand with 3 possible metal-binding sites, L-histidine has been studied for its copper complexing ability over several decades (13). Complexing to histidine delivers copper to an exchangeable blood pool and enhances copper uptake in cells

(27). By contrast, free copper binds albumin with high affinity, which is not as helpful for cellular copper uptake (28). In physiologic conditions, copper–histidine may contain copper in the 2+ state with 2 histidine species (13), whereas copper–histidine complexes may shift to Cu^{++} with 4 histidine species under freezing conditions, as shown by electron paramagnetic resonance (29). The copper–histidine complex may contain copper in the 1+ state as well (30). Recently, the radiographic structure of copper–histidine crystals showed coordination by 2 histidine species (31). Buffers, such as HEPES in our studies, do not complex copper to any significance (32).

In our studies, clearance of ^{64}Cu–histidine from the blood with uptake in the liver in LEA and LEC−/− rats was in agreement with entry of the complex into an exchangeable copper pool. ^{64}Cu entered the liver gradually, although more efficiently in LEC+/− and LEC−/− rats than in LEA rats. This result was similar to a previous study in which free ^{64}Cu instilled into the stomach was more rapidly cleared from the blood in LEC−/− rats, with greater accumulation in tissues (33). Whether chronic exposure to copper in LEC rats may increase copper uptake capacity is not known, but such may be a possibility.

After incorporation in the liver, ^{64}Cu was clearly transferred from the ^{64}Cu–histidine complex to *Atp7b* in view of biliary excretion in an *Atp7b*-dependent manner. Evidence has confirmed this process: ^{64}Cu was excreted in LEA and LEC+/− rats and not at all in LEC rats, in which *Atp7b* deficiency was the only known defect; acute or chronic liver injury did not alter ^{64}Cu excretion; increase in bile flow alone, that is, after sodium valproate (21), did not alter ^{64}Cu excretion; lack of an effect on ^{64}Cu excretion of hydrocortisone, which upregulated intracellular FK503-binding protein expression (22), and also increased copper efflux in ^{64}Cu-loaded cells by association with ATOX1 (23), were demonstrated; and restoration in LEC−/− rats of ^{64}Cu excretion after liver repopulation with healthy hepatocytes was shown. In healthy LEA rats, hepatic uptake of ^{64}Cu–histidine was followed by gradual copper excretion because 50% of the hepatic activity remained after 24 h. This result contrasted with slower excretion of free ^{64}Cu, requiring over 2 d for loss of 50% liver activity in healthy rats (9).

Our studies of ^{64}Cu excretion after reconstitution of *Atp7b* function by cell transplantation in LEC−/− rats were informative. In this situation, hepatic image analysis showed partial correction, likely due to continued ^{64}Cu accumulation in residual diseased hepatocytes. The balance between retention and loss of ^{64}Cu decreased the slope of hepatic SUV toward normal in 60 min but not to levels in healthy LEA rats. This finding was different from LEC +/− rats because each hepatocyte in heterozygous rats could rapidly excrete ^{64}Cu, compared with diseased hepatocytes without such capacity in LEC−/− rats. Therefore, *Atp7b* reconstitution substantiated that small-animal PET distinguished between stages of hepatic copper retention.

This ability to identify ^{64}Cu excretion without confounding by coincidental liver disease, fibrosis, inflammation, or changes in bile flow should be highly significant for diagnosing WD in clinical settings. The possibility of rapidly diagnosing WD by noninvasive imaging at any stage of life or disease will be of enormous significance. The hepatic SUV-max parameter with data acquired within 30–60 min of imaging should permit rapid diagnosis of WD or healthy states.

During publication of this work, small-animal PET studies with free ^{64}Cu were reported in an *Atp7b* knockout mouse model of WD (34). The findings were in agreement with our results. On the other hand, successful use of ^{64}Cu– histidine offers opportunities for targeting of radiotracers for improving results.

CONCLUSION

The complex of ^{64}Cu–histidine was cleared from the blood, incorporated in liver, and excreted in bile of healthy rats. In the LEC rat model of WD, ^{64}Cu–histidine was efficiently cleared from the blood with hepatic uptake, but ^{64}Cu was not excreted in bile. Reconstitution of *Atp7b* deficiency by transplantation of healthy cells confirmed that clearance of ^{64}Cu in LEC rats was due to *Atp7b*. Analysis of hepatic ^{64}Cu clearance by small-animal PET demonstrated that healthy and WD states were rapidly distinguished. This finding will advance molecular imaging for WD with ^{64}Cu complexes.

Acknowledgments

Small-animal PET was performed by Dr. Eugene Fine and Wade Koba at the Donald M. Blaufox Laboratory, Albert Einstein College of Medicine. This work was supported in part by NIH grants R01DK088561, R01DK071111, and P30 DK41296; by a grant from New York State Stem Cell Program; and by DFG, Germany, grant BA 3609/1-1. This study was published in part as the following abstracts: Bhargava KK et al. *Eur J Nucl Med Mol Imaging*. 2009;36 (suppl 2):S224 and Bahde R et al. *Hepatology*. 2009,50:749A.

REFERENCES

1. Ala A, Walker AP, Ashkan K, Dooley JS, Schilsky ML. Wilson's disease. Lancet. 2007; 369:397–408. [PubMed: 17276780]
2. Kim BE, Nevitt T, Thiele DJ. Mechanisms for copper acquisition, distribution and regulation. Nat Chem Biol. 2008; 4:176–185. [PubMed: 18277979]
3. Bull PC, Thomas GR, Rommens JM, Forbes JR, Cox DW. The Wilson disease gene is a putative copper transporting P-type ATPase similar to the Menkes gene. Nat Genet. 1993; 5:327–337. [PubMed: 8298639]
4. Irani AN, Malhi H, Slehria S, et al. Correction of liver disease following transplantation of normal hepatocytes in LEC rats modeling Wilson's disease. Mol Ther. 2001; 3:302–309. [PubMed: 11273771]
5. Malhi H, Joseph B, Schilsky ML, Gupta S. Development of cell therapy strategies to overcome copper toxicity in the LEC rat model of Wilson disease. Regen Med. 2008; 3:165–173. [PubMed: 18307400]
6. Joseph B, Kapoor S, Schilsky ML, Gupta S. Bile salt-induced pro-oxidant liver damage promotes transplanted cell proliferation for correcting Wilson disease in the Long-Evans Cinnamon rat model. Hepatology. 2009; 49:1616–1624. [PubMed: 19185006]
7. Ha-Hao D, Merle U, Hofmann C, et al. Chances and shortcomins of adenovirus-mediated ATP7B gene transfer in Wilson disease: proof of principle demonstrated in a pilot study with LEC rats. Z Gastroenterol. 2002; 40:209–216. [PubMed: 11961729]
8. Sternlieb I, Scheinberg IH. The role of radiocopper in the diagnosis of Wilson's disease. Gastroenterology. 1979; 77:138–142. [PubMed: 447011]
9. Owen CA Jr. Metabolism of radiocopper (Cu^{64}) in the rat. Am J Physiol. 1965; 209:900–904. [PubMed: 5849489]
10. Dunn MA, Green MH, Leach RM Jr. Kinetics of copper metabolism in rats: a compartmental model. Am J Physiol. 1991; 261:E115–E125. [PubMed: 1858867]
11. Gibbs K, Hanka R, Walshe JM. The urinary excretion of radiocopper in pre-symptomatic and symptomatic Wilson's disease, heterozygotes and controls: its significance in diagnosis and management. Q J Med. 1978; 47:349–364. [PubMed: 715173]
12. Schilsky ML, Irani AN, Gorla GR, Volenberg I, Gupta S. Biliary copper excretion capacity in intact animals: correlation between ATP7B gene function, hepatic mass and copper excretion. J Biochem Mol Toxicol. 2000; 14:210–214. [PubMed: 10789499]
13. Deschamps P, Kulkarni PP, Gautam-Basak M, Sarkar B. The saga of copper(II)–L-histidine. Coord Chem Rev. 2005; 249:895–909.

14. Wernimont AK, Huffman DL, Lamb AL, O'Halloran TV, Rosenzweig AC. Structural basis for copper transfer by the metallochaperone for the Menkes/Wilson disease proteins. Nat Struct Biol. 2000; 7:766–771. [PubMed: 10966647]
15. Wu J, Forbes JR, Chen HS, Cox DW. The LEC rat has a deletion in the copper transporting ATPase gene homologous to the Wilson disease gene. Nat Genet. 1994; 7:541–545. [PubMed: 7951327]
16. Ahmed S, Deng J, Borjigin J. A new strain of rat for functional analysis for PINA. Brain Res Mol Brain Res. 2005; 137:63–69. [PubMed: 15950762]
17. Yoshida Y, Tokusashi Y, Lee GH, Ogawa K. Intrahepatic transplantation of normal hepatocytes prevents Wilson's disease in Long-Evans Cinnamon Rats. Gastroenterology. 1996; 111:1654–1660. [PubMed: 8942746]
18. Joseph B, Bhargava KK, Trunco G, Kumaran V, Palestro CJ, Gupta S. Regulation of hepatobiliary transport activity and noninvasive identification of cytokine-dependent liver inflammation. J Nucl Med. 2005; 46:146–152. [PubMed: 15632045]
19. Joseph B, Bhargava KK, Tronco GG, Palestro CJ, Gupta S. Systemic and local release of inflammatory cytokines regulates hepatobiliary excretion of ^{99m}Tc-mebrofenin. Nucl Med Commun. 2008; 29:336–344. [PubMed: 18317297]
20. Bhargava KK, Joseph B, Ananthanarayanan M, et al. ATP-binding cassette subfamily C member 2 transports ^{99m}Tc-mebrofenin into bile and offers molecular pathway-specific liver imaging. J Nucl Med. 2009; 50:1140–1146. [PubMed: 19525466]
21. Kuzuya T, Amioka K, Nabeshima T. Valproic acid increases biliary copper excretion in the rat. Epilepsy Res. 2002; 51:279–285. [PubMed: 12399078]
22. Vermeer H, Hendriks-Stegeman BI, van der Burg B, van Buul-Offers SC, Jansen M. Glucocorticoid-induced increase in lymphocytic FKBP51 messenger ribonucleic acid expression: a potential marker for glucocorticoid sensitivity, potency, and bioavailability. J Clin Endocrinol Metab. 2003; 88:277–284. [PubMed: 12519866]
23. Sanokawa-Akakura R, Dai H, Akakura S, Weinstein, Fajardo JE, Lang SE, Wadsworth S, Siekierka J, Birge RB. A novel role for the immunophilin FKBP52 in copper transport. J Biol Chem. 2004; 279:27845–27848. [PubMed: 15133031]
24. Krohn N, Kapoor S, Enami Y, et al. Hepatocyte transplantation-induced liver inflammation is driven by cytokines-chemokines associated with neutrophils and Kupffer cells. Gastroenterology. 2009; 136:1806–1817. [PubMed: 19422086]
25. Benten D, Kumaran V, Joseph B, et al. Hepatocyte transplantation activates hepatic stellate cells with beneficial modulation of cell engraftment in rats. Hepatology. 2005; 42:1072–1081. [PubMed: 16250034]
26. Hung IH, Suzuki M, Yamaguchi Y, Yuan DS, Klausner RD, Gitlin JD. Biochemical characterization of the Wilson disease protein and functional expression in the yeast Saccharomyces cerevisiae. J Biol Chem. 1997; 272:21461–21466. [PubMed: 9261163]
27. Bingham MJ, McArdle HJ. A comparison of copper uptake by liver plasma membrane vesicles and uptake by isolated cultured rat hepatocytes. Hepatology. 1994; 20:1024–1031. [PubMed: 7927204]
28. McArdle HJ, Guthrie JR, Ackland ML, Danks DM. Albumin has no role in the uptake of copper by human fibroblasts. J Inorg Biochem. 1987; 31:123–131. [PubMed: 2828539]
29. Basosi R, Valensin G, Gaggelli E, et al. Multifrequency ESR of Cu(II)-(His), (His 5 Histidine). 1. Immobile Phase. Inorg Chem. 1986; 25:3006–3010.
30. Venelinov T, Arpadjan S, Karadjova I, Beattie J. Properties of the copper(II)-histidine complex obtained after dialysis of human plasma with histidine. Acta Pharm. 2006; 56:105–112. [PubMed: 16613740]
31. Deschamps P, Kulkarni PP, Sarkar B. X-ray structure of physiological copper (II)−bis(l-histidinato) complex. Inorg Chem. 2004; 43:3338–3340. [PubMed: 15154794]
32. Vasconcelos MTSD, Almeida CMR. Electrochemical study of proton ionisation, copper(II) complexation and surfactant properties of piperazine-N-N'-bis[2-hydroxypropanesulfonic acid] pH buffer: comparison with other N-substituted aminosulfonic acids pH buffers. Anal Chim Acta. 1998; 369:115–122.

33. Bissig KD, Honer M, Zimmermann K, Summer KH, Solioz M. Whole animal copper flux assessed by positron emission tomography in the Long–Evans cinnamon rat: a feasibility study. Biometals. 2005; 18:83–88. [PubMed: 15865413]

34. Peng F, Lutsenko S, Sun X, Muzik O. Positron emission tomography of copper metabolism in the Atp7b (−/−) knock-out mouse model of Wilson's disease. Mol Imaging Biol. 2012; 14:70–78. [PubMed: 21327972]

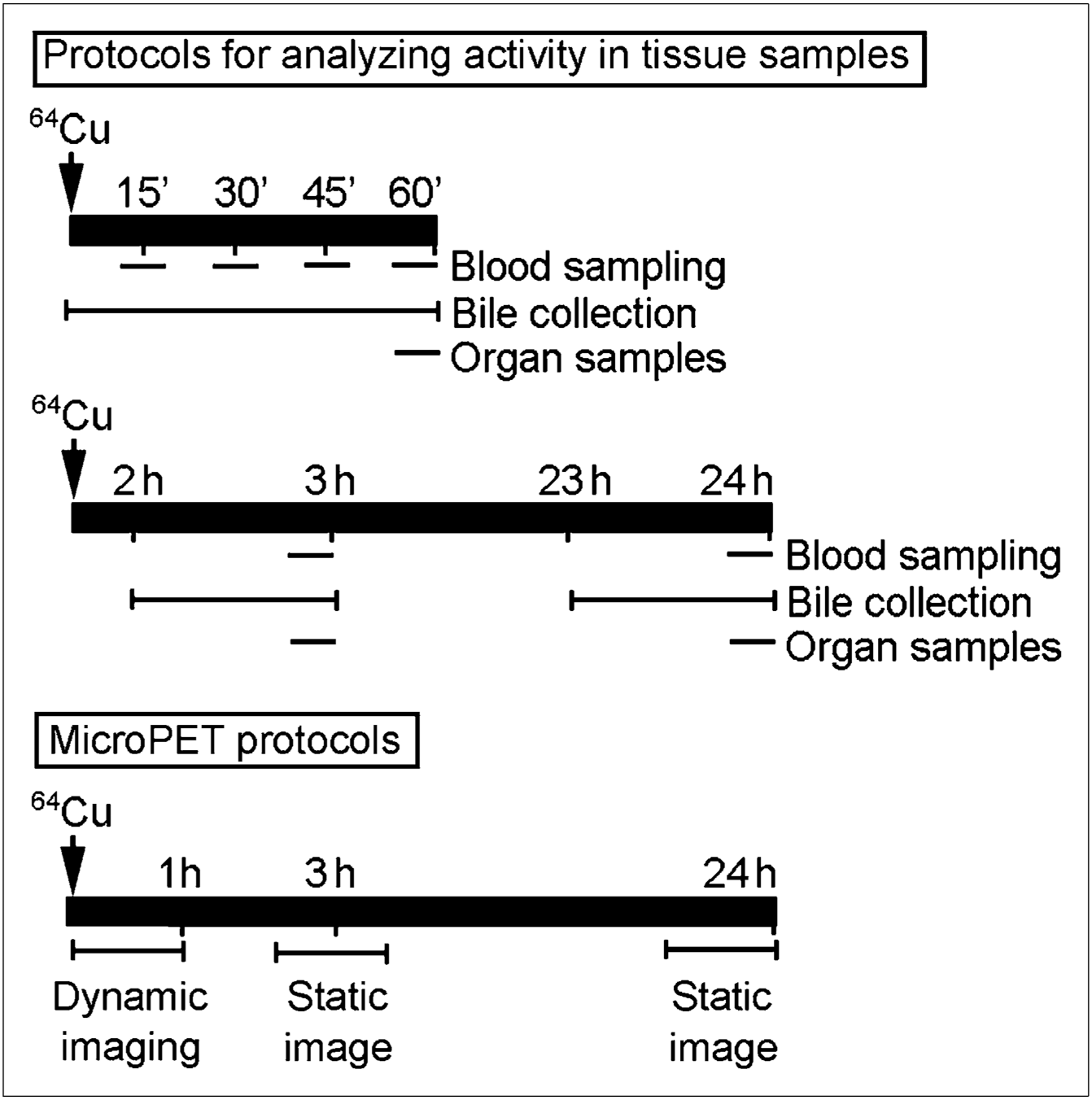

Figure 1.
Experimental design. Protocols for analyzing ^{64}Cu activity by γ-counting in blood and bile samples are shown, including longer-term studies with bile collection and blood and tissue sampling. Protocols for small-animal PET are shown at bottom to indicate dynamic imaging in first hour and static imaging 3 and 24 h after ^{64}Cu–histidine.

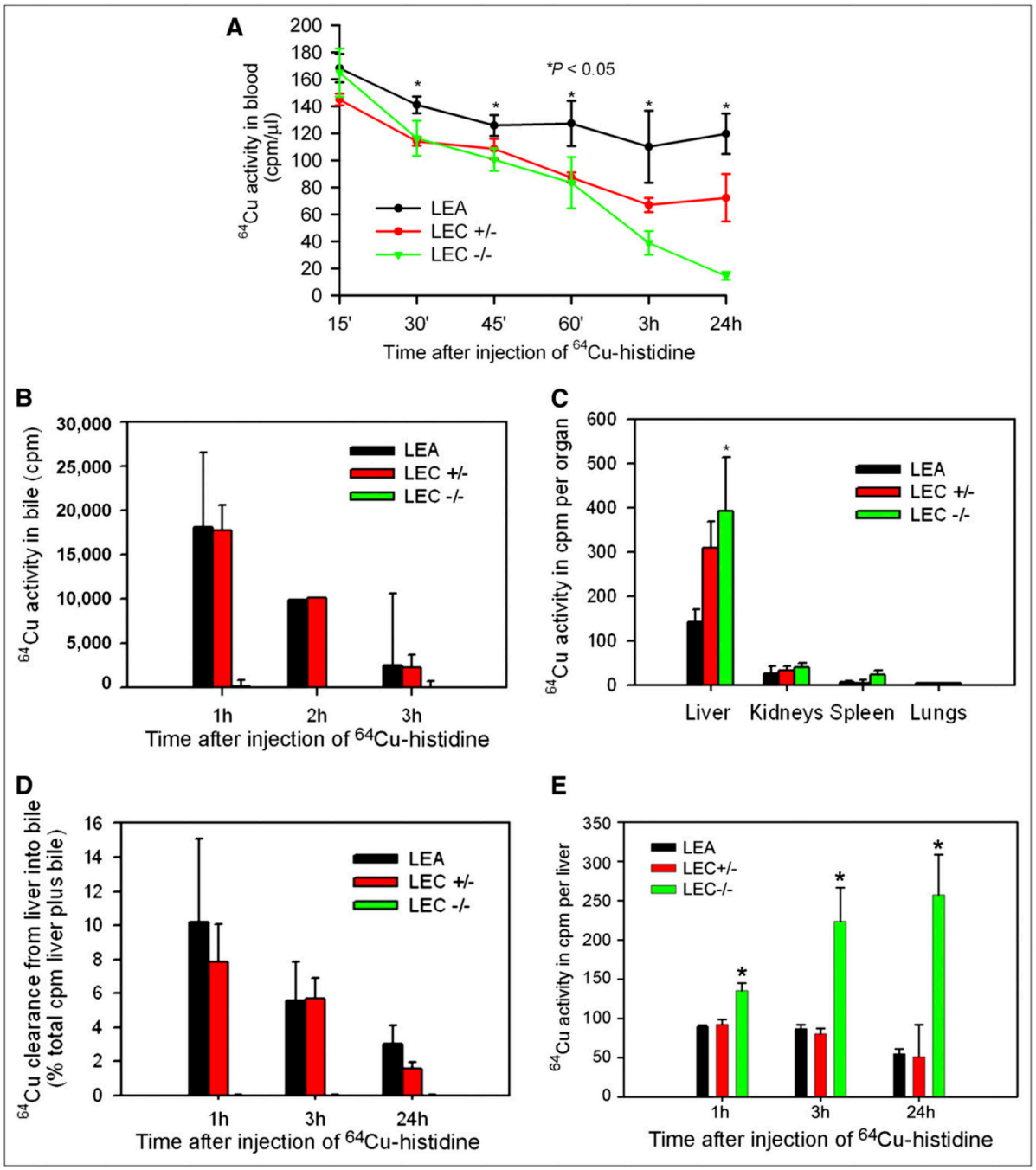

Figure 2.

^{64}Cu–histidine handling. (A) ^{64}Cu–histidine clearance from blood in LEC+/−, LEC−/−, and LEA rats. (B) Uptake of ^{64}Cu–histidine in liver and other organs. (C) Bile ^{64}Cu excretion in LEA, LEC+/−, and LEC−/− rats. (D) ^{64}Cu excretion in bile as percentage of liver plus bile activity. (E) ^{64}Cu activity in organs 1, 3, and 24 h after ^{64}Cu–histidine was given. Asterisks indicate $P < 0.05$ vs. LEA and LEC+/− rats. *$P < 0.05$, ANOVA.

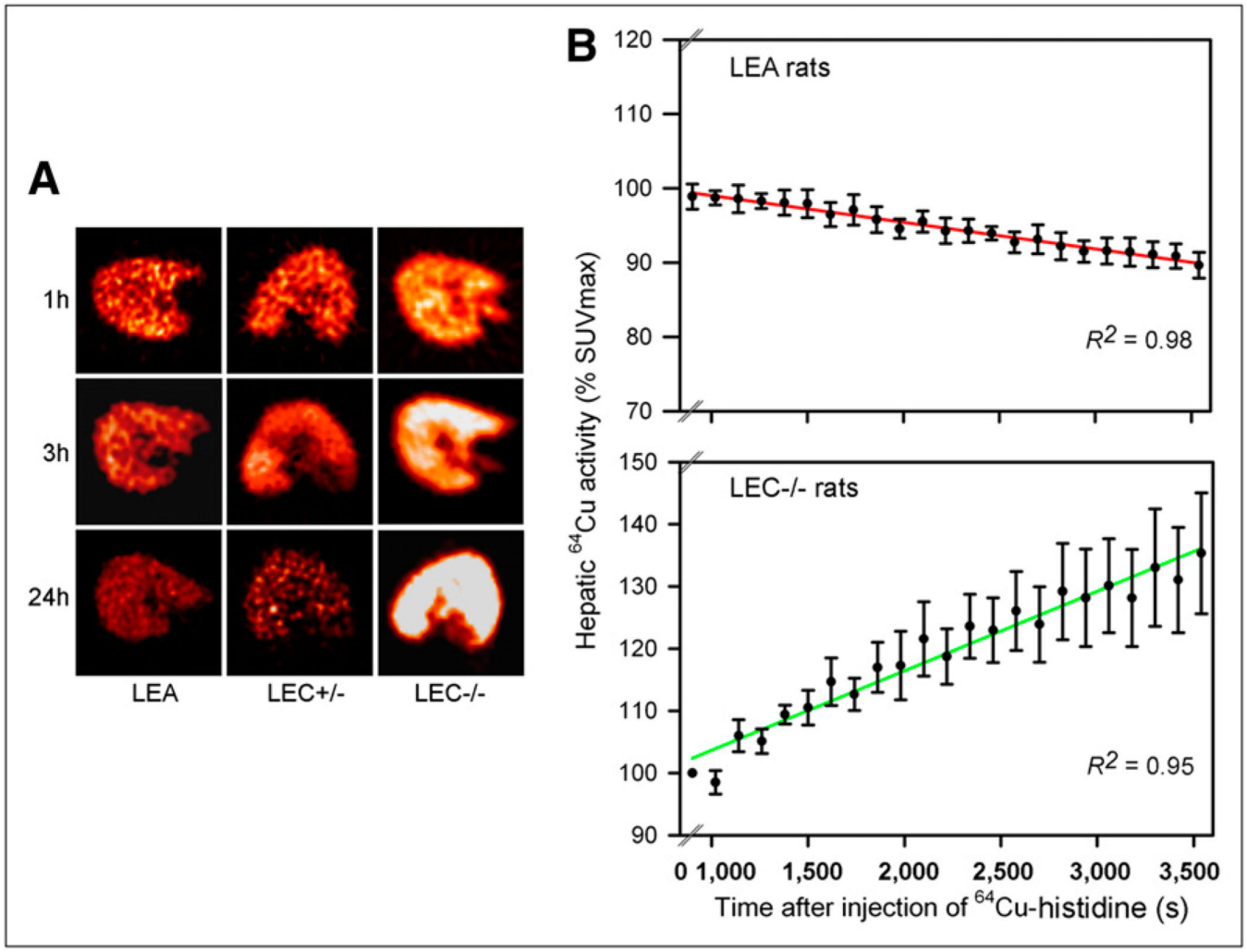

Figure 3.

Imaging for tissue ^{64}Cu activity. (A) Liver small-animal PET images from rats 1, 3, and 24 h after ^{64}Cu–histidine showing that activity decreased over time in LEA and LEC+/− rats and increased in LEC rats. (B) Hepatic SUV generated by linear regression over 1 h after ^{64}Cu–histidine in LEA and LEC−/− rats.

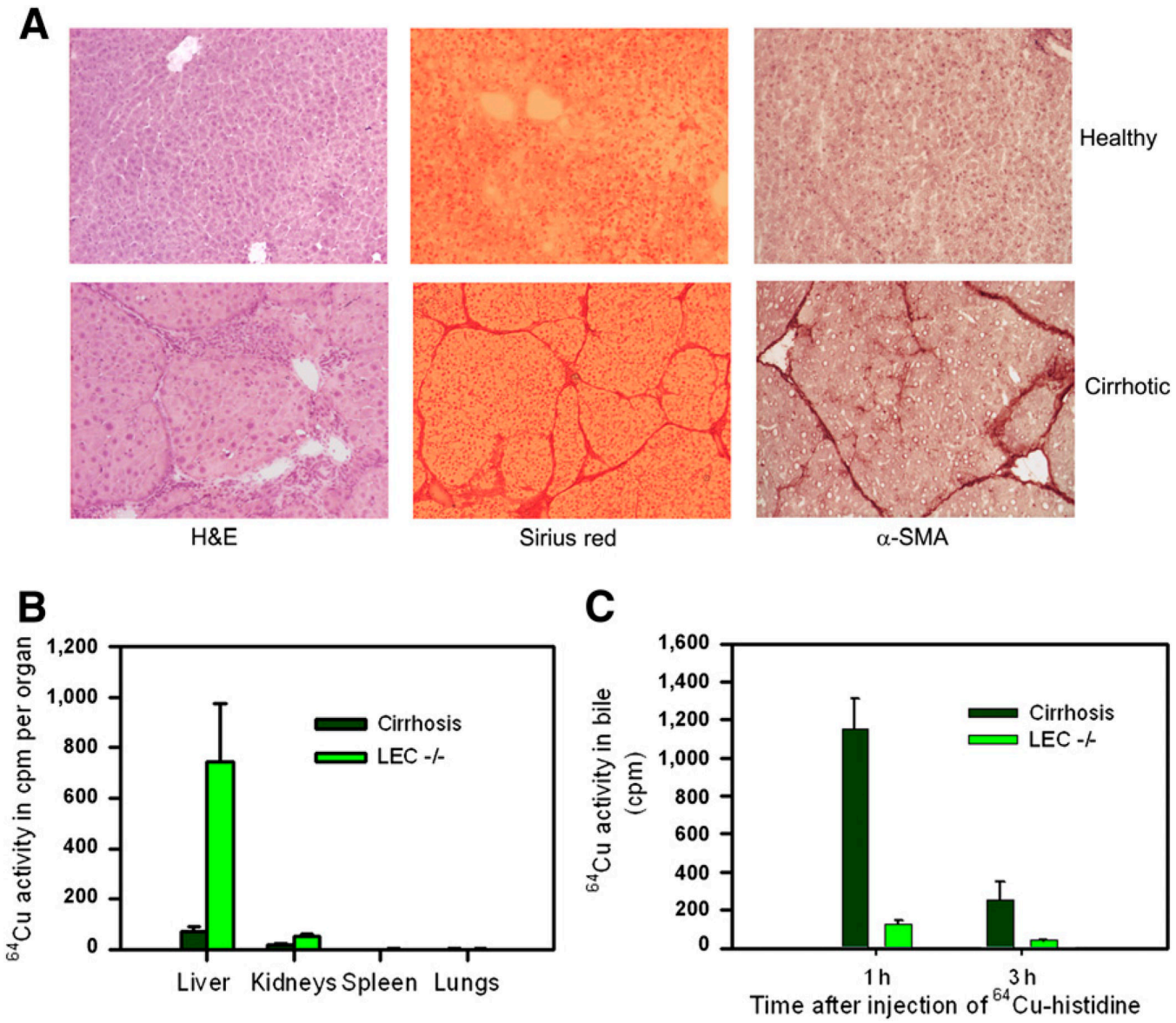

Figure 4.

^{64}Cu handling in rats with cirrhosis vs. LEC−/− rats. (A) Liver histology in healthy rats and cirrhotic rats after phenobarbitone plus repeated CCl_4 for 3 mo (×100). (B) ^{64}Cu activity in organs 3 h after injection of ^{64}Cu–histidine. (C) ^{64}Cu excretion in bile of cirrhotic rats versus LEC−/− rats. α-SMA = α-smooth muscle actin; H&E = hematoxylin and eosin.

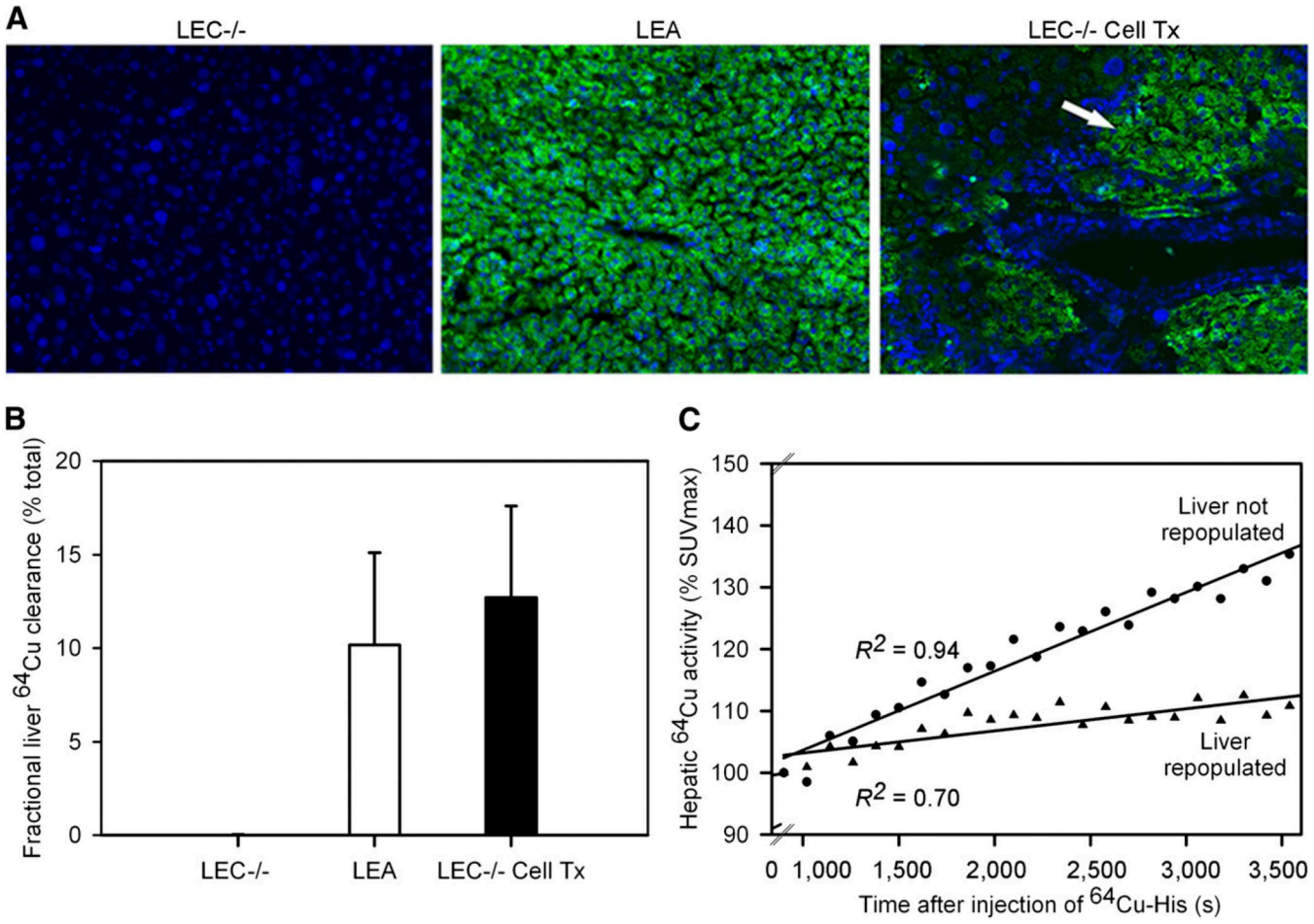

Figure 5.

Copper excretion in LEC−/− rats after reconstitution of hepatic *Atp7b* with transplanted healthy LEA hepatocytes. LEC−/− rats are shown 3–12 mo after cell transplantation. (A) Immunostaining for hepatic *Atp7b* in untreated control LEC−/− rat, healthy donor LEA rat, and LEC−/− rat with areas of transplanted hepatocytes containing *Atp7b* (arrow, panel on right) (×100; 4′,6-diamidino-2-phenylindole counterstain of nuclei). (B) Bile ^{64}Cu excretion over 1 h in untreated control LEC−/− rats, healthy LEA rats, and LEC−/− rats after transplantation of LEA rat hepatocytes. (C) Analysis of hepatic ^{64}Cu activity by small-animal PET during 1 h in representative animals. Tx = therapy.

TABLE 1

Distribution of Animals in Various Studies

Experimental purpose	Animal groups	Measurements made
^{64}Cu handling in first hour	LEA rats (n = 15)	Tail vein (n = 3) or intrasplenic injection of ^{64}Cu (n = 12)
	LEC+/− rats (n = 15)	Blood sampling at 15, 30, 45, and 60 min
	LEC−/− rats (n = 15)	Bile collection × 60 min
		Tissue sampling
^{64}Cu handling over 2–24 h	LEA rats (n = 15)	Blood sampling at 2, 3, and 24 h
	LEC+/− rats (n = 9)	Bile collection × 60 min after 2, 3, and 24 h
	LEC−/− rats (n = 9)	Tissue sampling
Small-animal PET studies	LEA rats (n = 9)	Imaging at 1, 3, and 24 h
	LEC+/− rats (n = 9)	Bile collection × 60 min after 1, 3, and 24 h
	LEC−/− rats (n = 9)	Tissue sampling
Liver injury and ^{64}Cu handling	Healthy LEA rats (n = 6)	^{99m}Tc-mebrofenin imaging
	LEA rats, acute injury (n = 6)	Blood sampling at 15, 30, 45, and 60 min and 3 h
	F344 rats, chronic injury (n = 9)	Bile collection × 60 min after 1 and 3 h
		Tissue sampling
Effect of drugs on ^{64}Cu excretion	LEA rats, valproic acid (n = 6)	Bile collection × 60 min
	LEA rats, hydrocortisone (n = 3)	Tissue sampling
Cell transplantation studies	LEC rats (n = 10)	Bile collection × 60 min
		Tissue sampling
		Small-animal PET